Electronic Supplementary Information

Ultrahigh-voltage integrated micro-supercapacitors with designable shapes and superior flexibility

Xiaoyu Shi,‡[abc] Songfeng Pei,‡[d] Feng Zhou,[a] Wencai Ren,*[d] Hui-Ming Cheng,[de] Zhong-Shuai Wu*[a] and Xinhe Bao[ab]

[a]Dalian National Laboratory for Clean Energy, Dalian Institute of Chemical Physics, Chinese Academy of Sciences, 457 Zhongshan Road, Dalian 116023, China.
[b]State Key Laboratory of Catalysis, Dalian Institute of Chemical Physics, Chinese Academy of Sciences, 457 Zhongshan Road, Dalian 116023, China.
[c]Department of Chemical Physics, University of Science and Technology of China, 96 JinZhai Road, Hefei 230026, P. R. China.
[d]Shenyang National Laboratory for Materials Science, Institute of Metal Research, Chinese Academy of Sciences, 72 Wenhua Road, Shenyang 110016, P. R. China.
[e]Tsinghua-Berkeley Shenzhen Institute, 1001 Xueyuan Road, Shenzhen 518055, China.
‡: These authors have equally contributed to this work.
E-mails: wcren@imr.ac.cn; wuzs@dicp.ac.cn.

Experimental Section

Preparation of SPG Ink

The graphene powder (Deyang Carbonene Technology Co., Ltd) and carbon black powder with a weight ratio of 7:3 was first mixed by high-speed agitator, and then added into the P-VC/VAc resin (E22/48a, Wacker Chemie) dissolved in DBE solution (DowDuPont) (P-VC/VAc: DBE weight ratio of 1:9) and milled by high-energy ball-milling at a speed of 500 r/min for 10 hours. After separation from the milling balls, the black thick liquid can be directly used as the ink for screen-printing. The solid content of prepared ink is ~35%.

Fabrication of SPG-IMSCs

Typically, a piece of PET film was placed about 5 mm below the printing screen with patterned mesh. Then, the SPG ink was positioned on the blank part of the screen. Through the screen, a squeegee was impelled with a speed of about 3 cm s^{-1} along surface of the screen to extrude ink for the deposition onto the placed substrate. After screen removal and drying of the patterned ink at 100 ^{o}C for 12 h, a polymer gel electrolyte of H_3PO_4/PVA (or ionic liquid) was carefully dropped to cover the project area of SPG microelectrodes and solidified for 12 hours. Finally, the SPG-IMSCs on a PET substrate were obtained. Similarly, SPG-IMSCs were prepared on other substrates, e.g., glass, A4 paper and cloth.

Material and Electrochemical Characterization

Materials characterization was conducted by SEM (JEOL JSM-7800F), TEM (JEM-2100), atomic force microscopy (AFM, Bruker, Dimension FastScan with ScanAsyst^{TM}), X-ray diffraction (XRD, X'pert Pro), Raman spectroscopy (LabRAM HR 800 Raman spectrometer, 632 nm). 3D profiles of SPG-MSCs was examined by surface profiler (KLA-Tencor Alphastep D-600). Viscosity of ink was tested by rotary viscosimeter (NDJ-5S). Electrical conductivity was tested by a 4-point probes resistivity measurement system (RST-9). Electrochemical performance of the SPG-MSCs and SPG-IMSCs was evaluated by CV measurements at different scan rates from 5 to 500 mV s^{-1}, GCD profiles conducted at different current densities from 0.01 to 0.2 mA cm^{-2}, and electrochemical impedance spectroscopy recorded in the frequency range from 0.01 Hz to 100 kHz with a 5 mV ac amplitude, using an electrochemical workstation (CHI 760E). High-voltage SPG-IMSCs consisting of in-series 130 cells was tested by Keithley Model 2450.

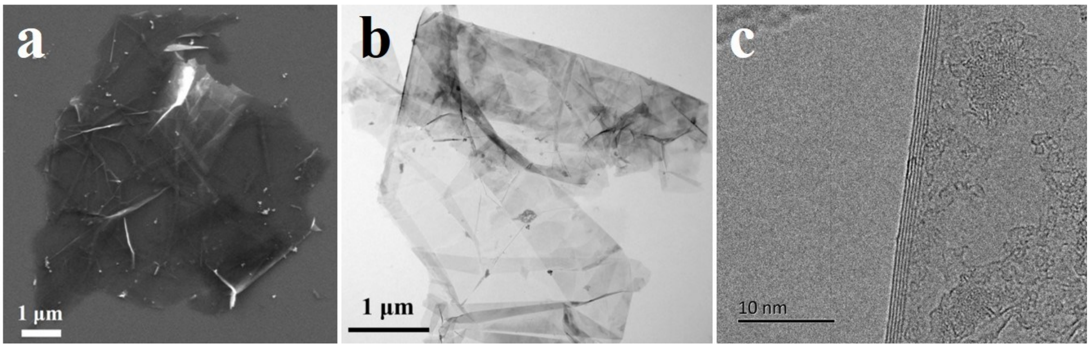

Fig. S1. Characterization of graphene nanosheets used for ink preparation. (a) SEM, (b) TEM and (c) HRTEM images of graphene nanosheet, showing the lateral size of ~6 µm and number of less than 5 layers.

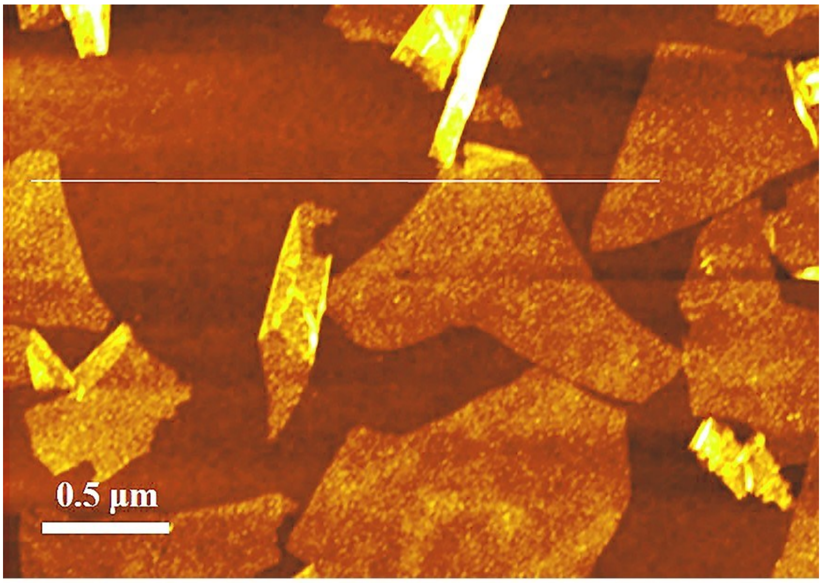

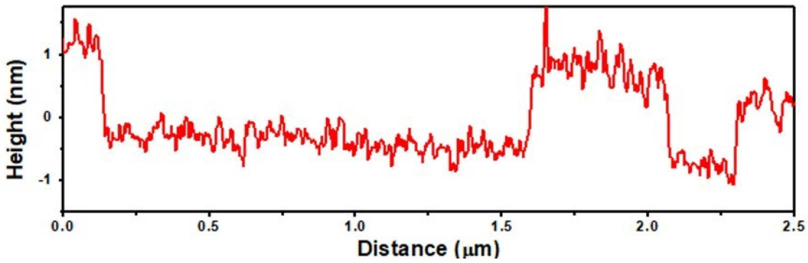

Fig. S2. AFM image (top) and height profile (bottom) of graphene nanosheets. The height profile reveraled a typical thickness of ~1.5 nm, corresponding to double-layer graphene.

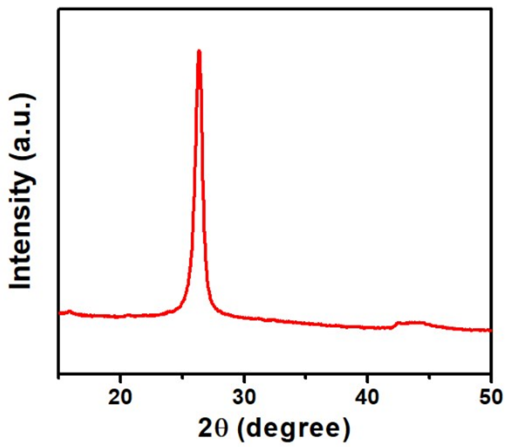

Fig. S3. XRD pattern of graphene nanosheets, identifying the layered structure of graphene nanosheets, with a typical interlayer spacing of 3.4 Å at 2θ of 26.4°.

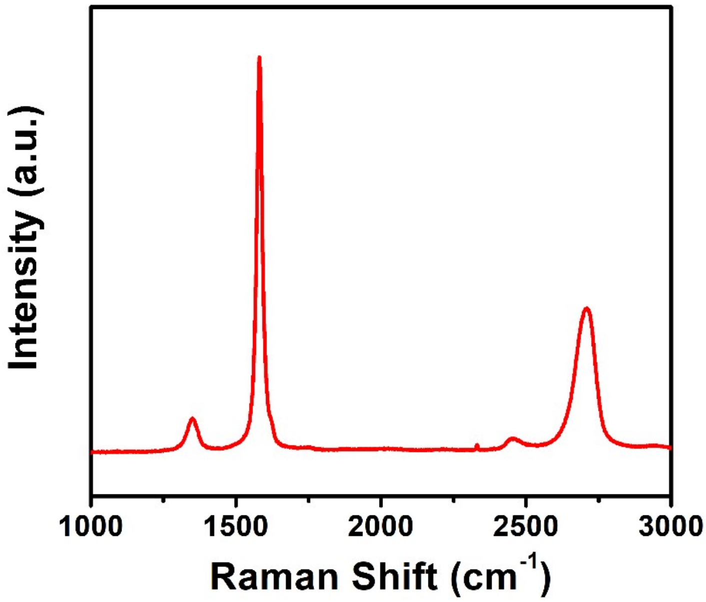

Fig. S4. Raman spectrum of graphene nanosheets. A high ratio ~9.4 of G peak to D peak demonstrated high quality of graphene nanosheets.

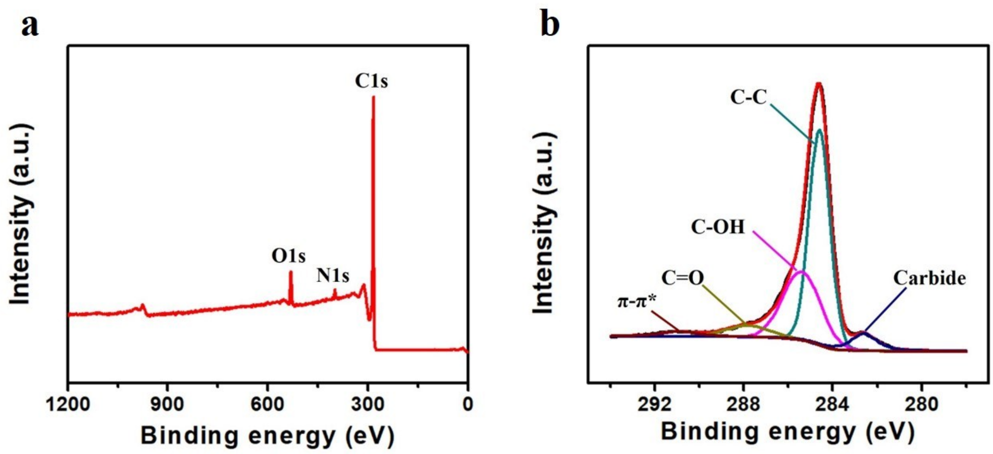

Fig. S5. (a) Full XPS and (b) C1s XPS spectra of graphene nanosheets, revealing the chemical composition of graphene.[1-4]

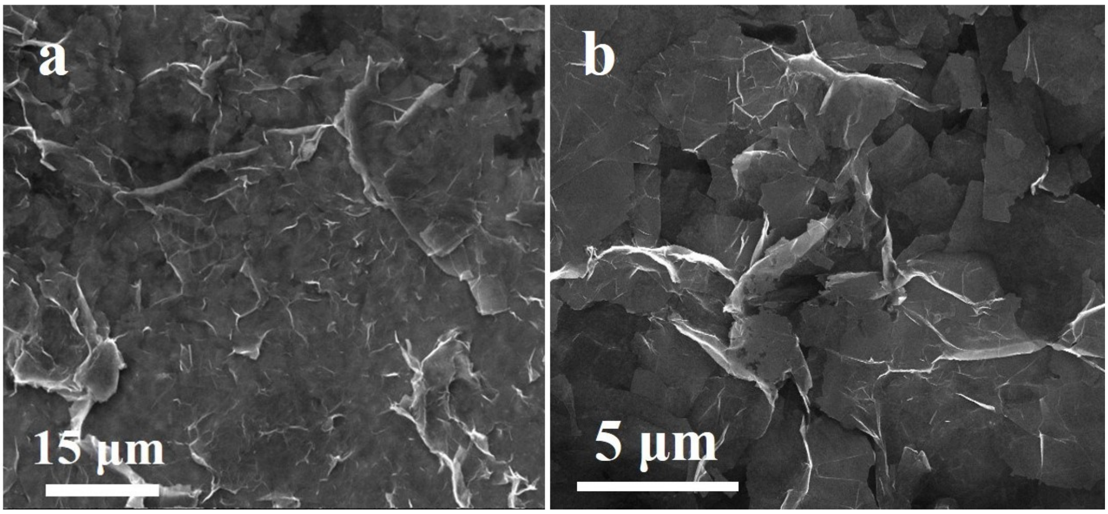

Fig. S6. (a,b) Top-view SEM images of SPG films, indicative of uniform distribution of graphene and formation of conductive network.

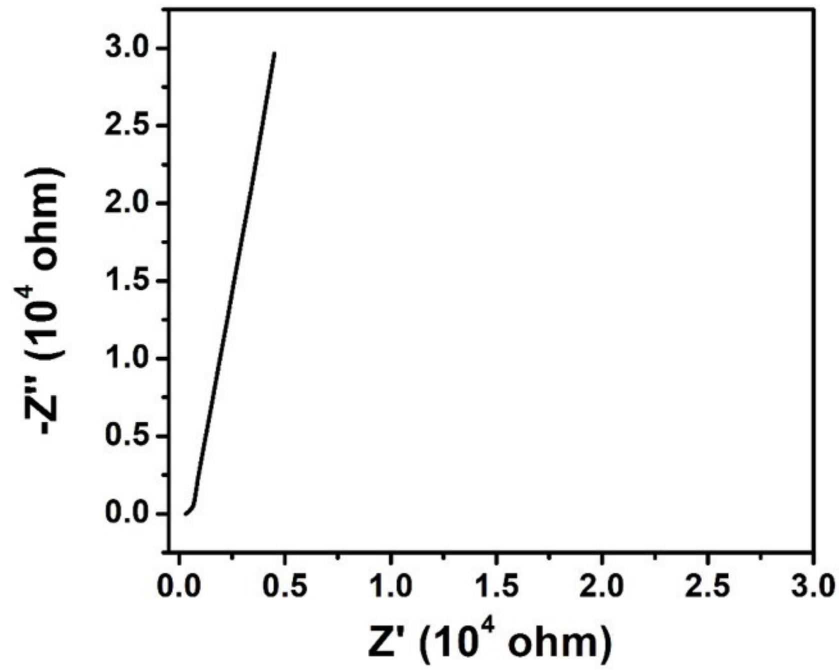

Fig. S7. The complex plane plot of interdigital SPG-MSCs in PVA/H_3PO_4 electrolyte.

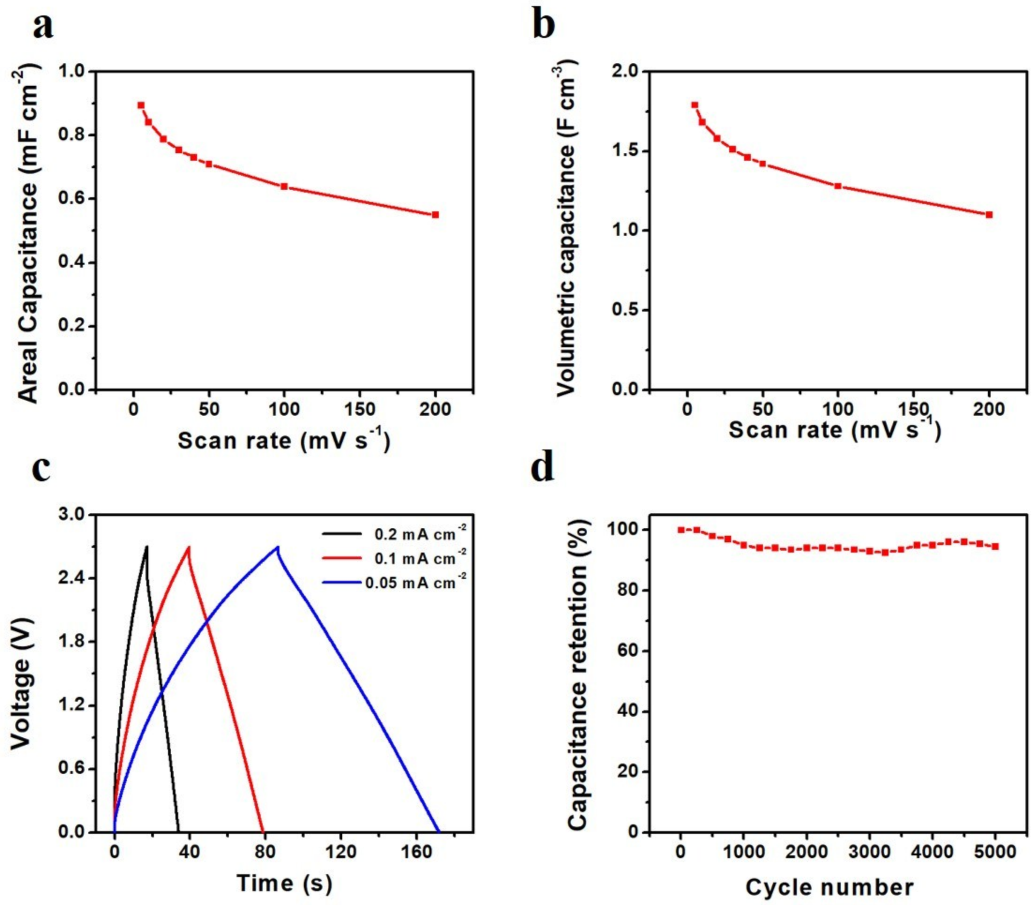

Fig. S8. Electrochemical performance of interdigital SPG-MSCs in $EMIMNTF_2$ electrolyte. (a) Areal capacitance and (b) volumetric capacitance as a function of scan rate. (c) GCD profiles of SPG-MSCs at varying current densities of 0.2, 0.1 and 0.05 mA cm^{-2}. (d) Cycling stability of SPG-MSCs for 5000 cycles at a current density of 0.3 mA cm^{-2}.

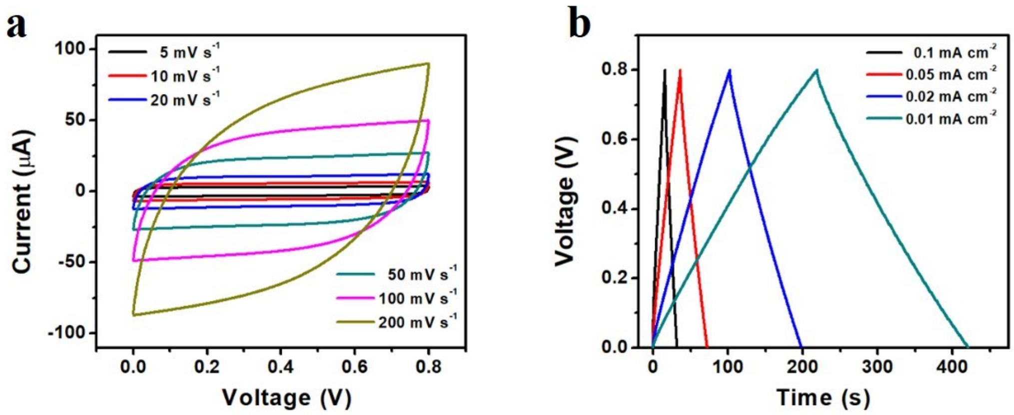

Fig. S9. SPG-MSCs with interdigital geometry screen printed on glass substrate. (a) CV curves of SPG-MSCs in PVA/H_3PO_4 electrolyte. (b) GCD profiles of SPG-MSCs in PVA/H_3PO_4 electrolyte. Both CV and GCD tests showed remarkable electrochemical performance, similar to the cell printed on PET substrate, indicative of wide applicability of our technique.

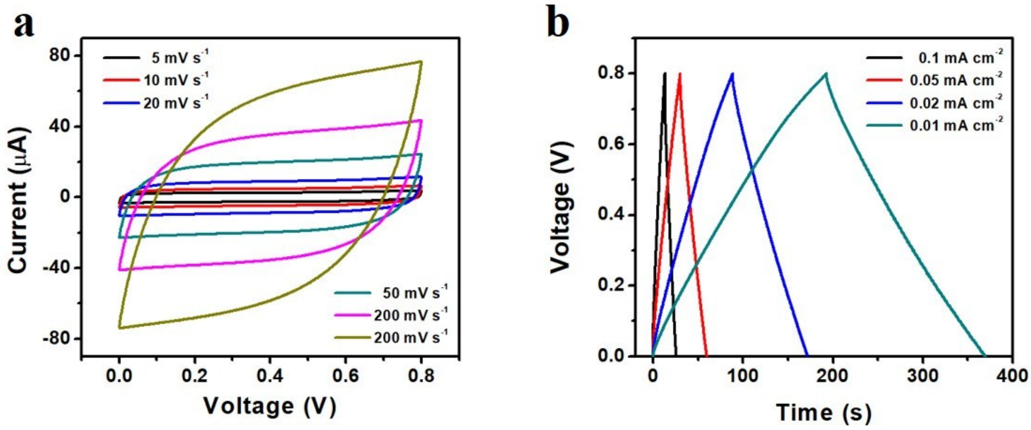

Fig. S10. SPG-MSCs with interdigital geometry screen printed on A4 paper. (a) CV curves of SPG-MSCs in PVA/H_3PO_4 electrolyte. (b) GCD profiles of SPG-MSCs in PVA/H_3PO_4 electrolyte. Both CV and GCD tests showed impressive electrochemical performance, similar to the cell printed on PET substrate, indicative of wide applicability of our technique.

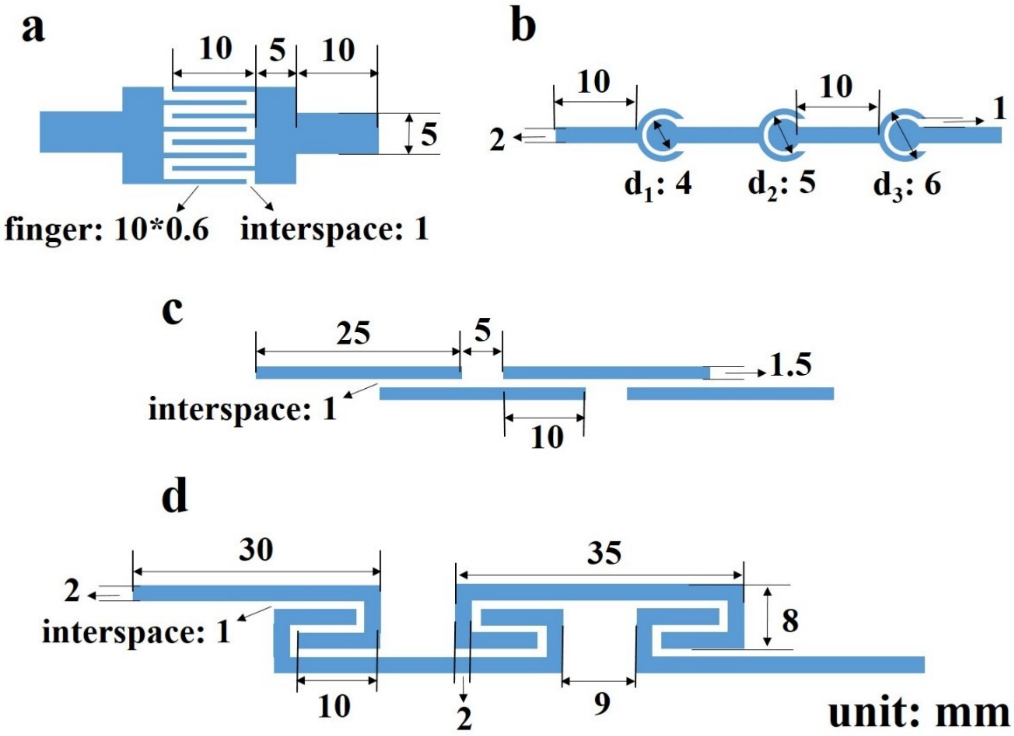

Fig. S11. Microelectrode size parameters of shape-designable SPG-MSCs with various geometries including (a) interdigital, (b) concentric, (c) linear and (d) foldable shapes.

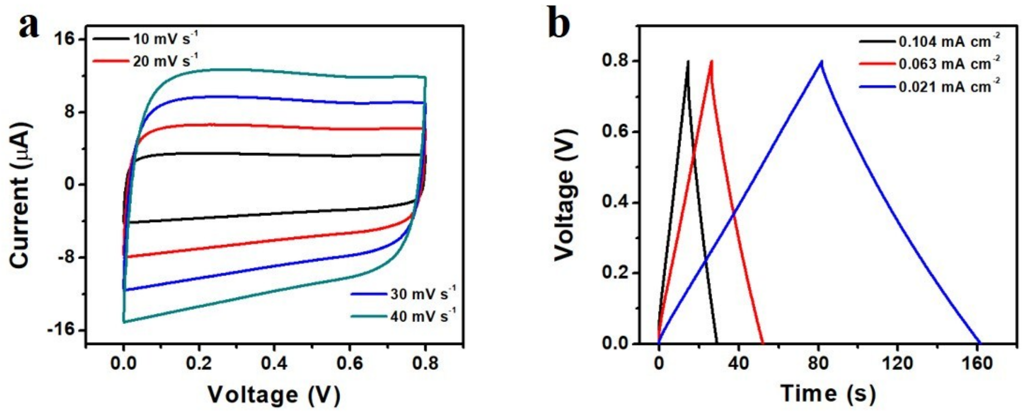

Fig. S12. CV curves and GCD profiles of SPG-MSCs with concentric geometry, tested in PVA/H_3PO_4 electrolyte.

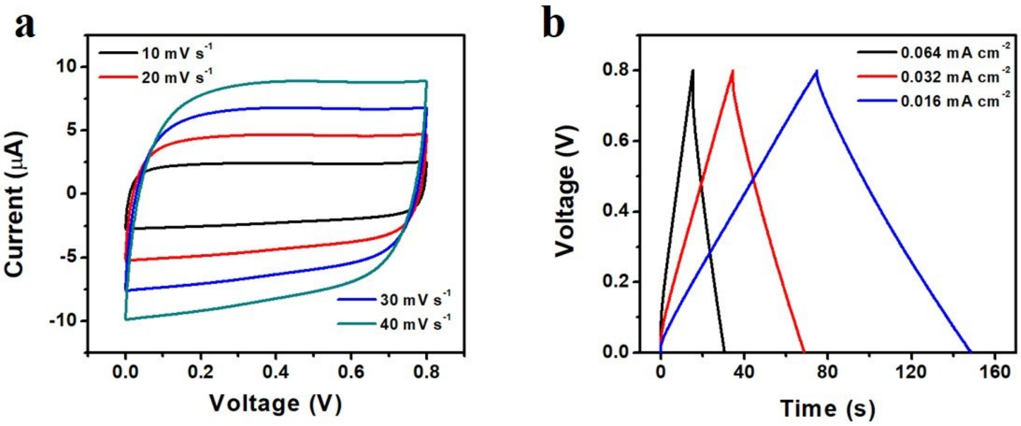

Fig. S13. CV curves and GCD profiles of SPG-MSCs with linear geometry, tested in PVA/H_3PO_4 electrolyte.

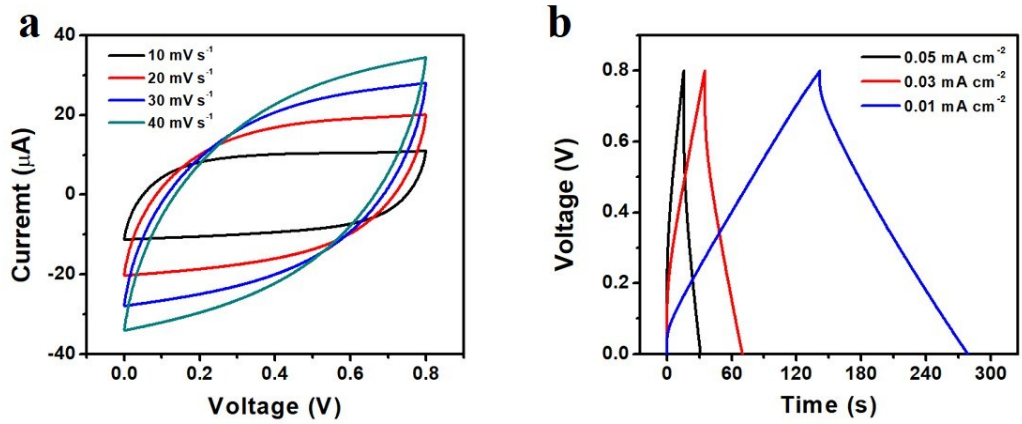

Fig. S14. CV curves and GCD profiles of SPG-MSCs with foldable geometry, tested in PVA/H_3PO_4 electrolyte. It is revealed that from Fig. S12 to S14 the in-plane device geometry plays an important role in electrochemical performances.

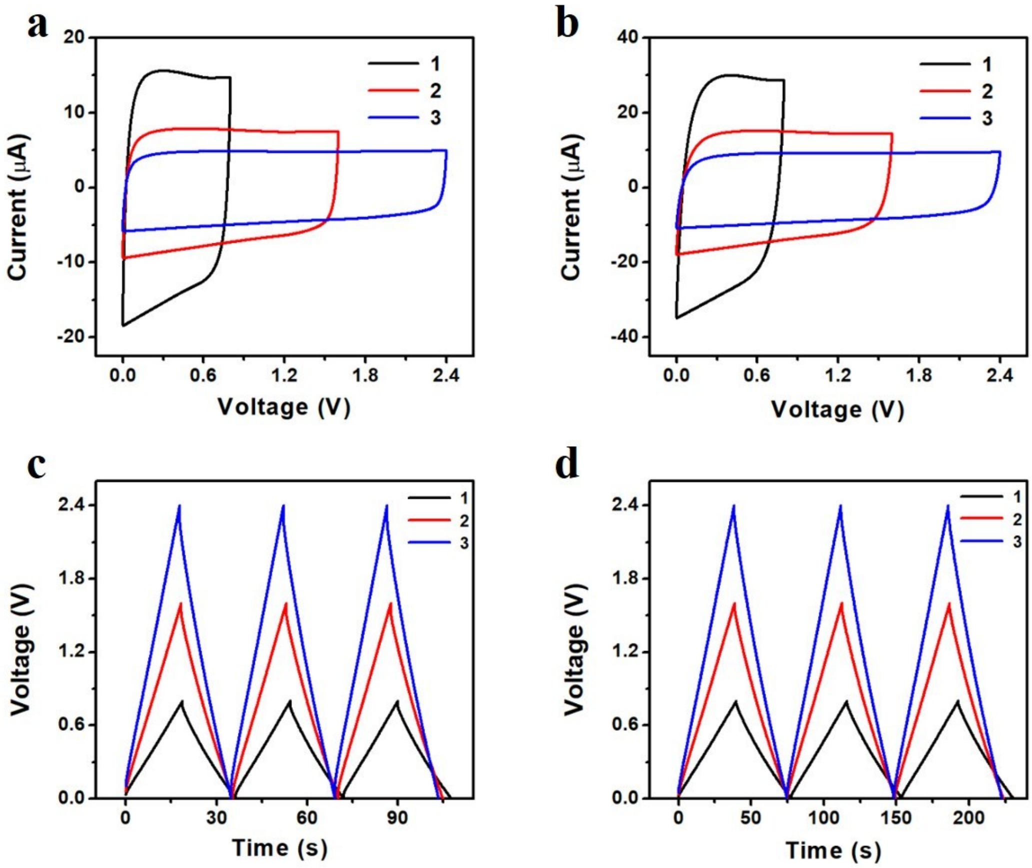

Fig. S15. Electrochemical performance of SPG-IMSCs with concentric geometry in PVA/H_3PO_4 electrolyte. CV curves of SPG-IMSCs with different number of serial cells, obtained at scan rates of (a) 50 and (b) 100 mV s^{-1}. GCD profiles of SPG-IMSCs with different number of serial cells, measured at current densities of (c) 0.083 and (d) 0.042 mA cm^{-2}.

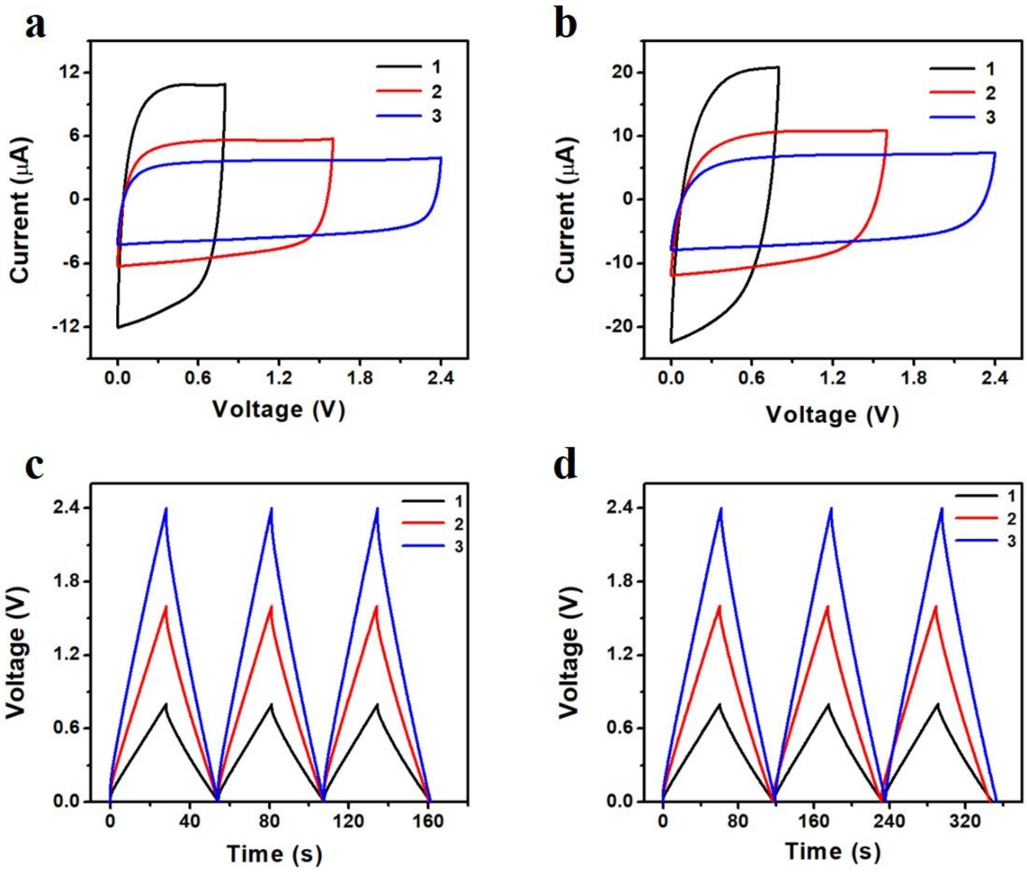

Fig. S16. Electrochemical performance of SPG-IMSCs with linear geometry in PVA/H_3PO_4 electrolyte. CV curves of SPG-IMSCs with different number of serial cells, obtained at scan rates of (a) 50 and (b) 100 mV s^{-1}. The corresponding GCD profiles tested at current densities of (c) 0.05 and (d) 0.025 mA cm^{-2}.

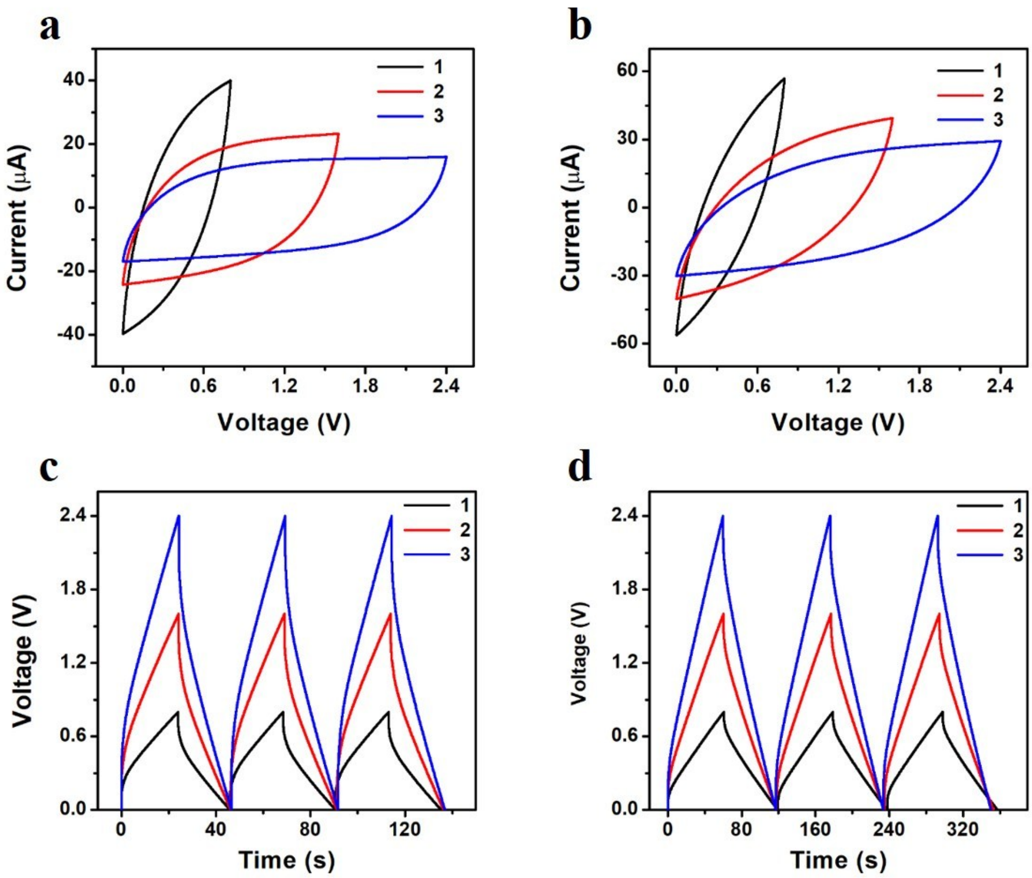

Fig. S17. Electrochemical performance of SPG-IMSCs with foldable geometry in PVA/H_3PO_4 electrolyte. CV curves of SPG-IMSCs with different number of serial cells, obtained at scan rates of (a) 50 and (b) 100 mV s^{-1}. GCD profiles of SPG-IMSCs with different number of serial cells, tested at current densities of (c) 0.04 and (d) 0.02 mA cm^{-2}. Fig. S15 to S17 demonstrate ideal tandem capacitive behaviors of our SPG-IMSCs.

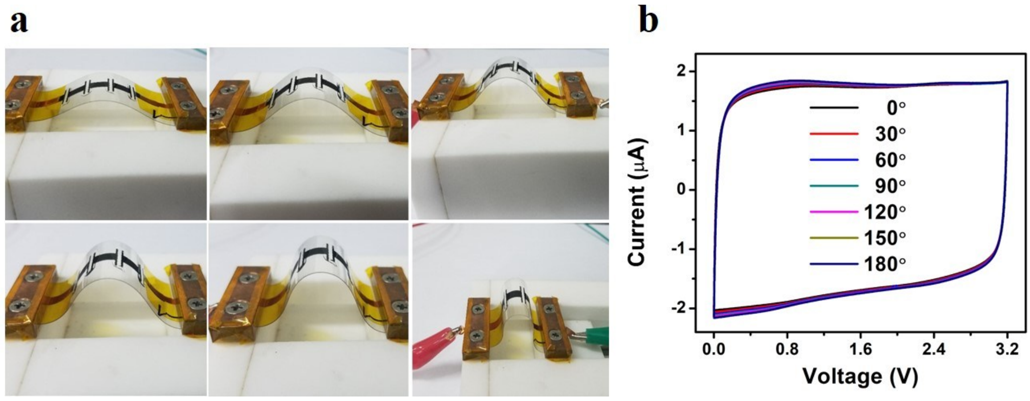

Fig. S18. Flexibility test of SPG-IMSCs with parallel strip geometry. (a) A photograph and (b) CV curves obtained at a scan rate of 50 mV s^{-1} of SPG-IMSCs under different bending angles. The almost overlapped CV curves indicated remarkable flexibility of our SPG-IMSCs.

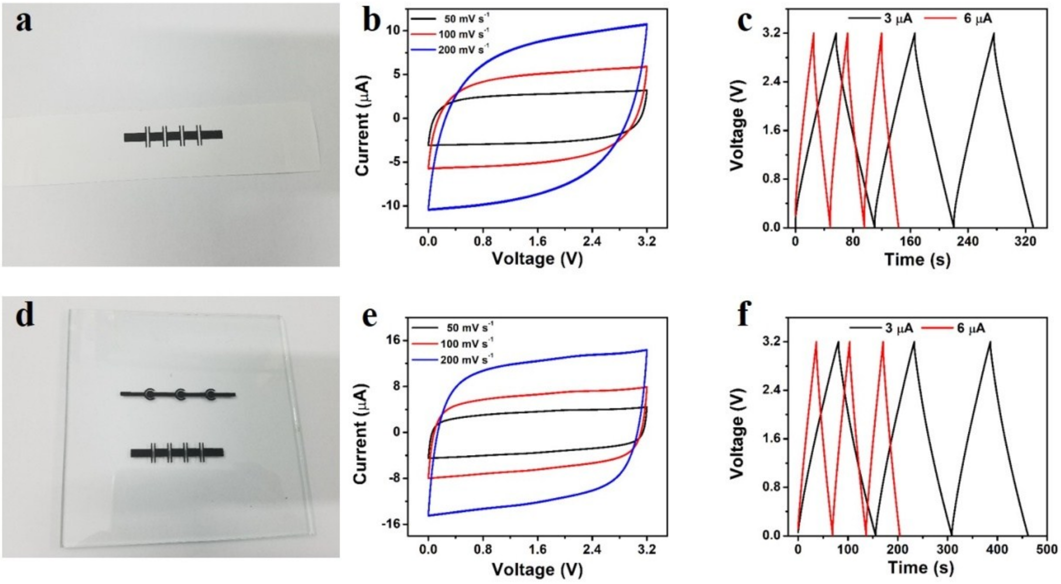

Fig. S19. Electrochemical performances of tandem SPG-IMSCs with parallel strip geometry. (a) Photographs, (b) CV curves and, (c) GCD profiles of four serially connected SPG-MSCs on A4 paper substrate. (d) Photographs, (e) CV curves and, (f) GCD profiles of four serially-connected SPG-MSCs on glass substrate.

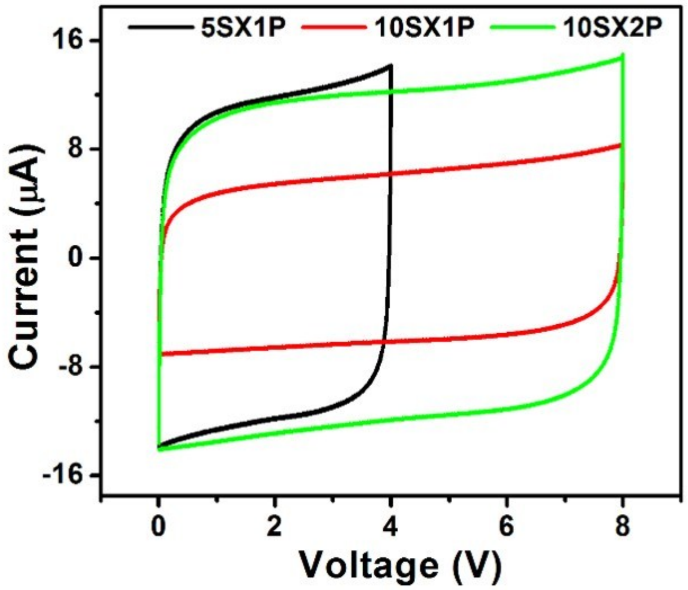

Fig. S20. CV curves of SPG-IMSCs connected in a serial and parallel fashion of 5S×1P, 10S×1P, and 10S×2P. The approximately equal current of SPG-IMSCs (5S×1P) and SPG-IMSCs (10S×2P) manifested outstanding performance uniformity of our integrated microdevices.

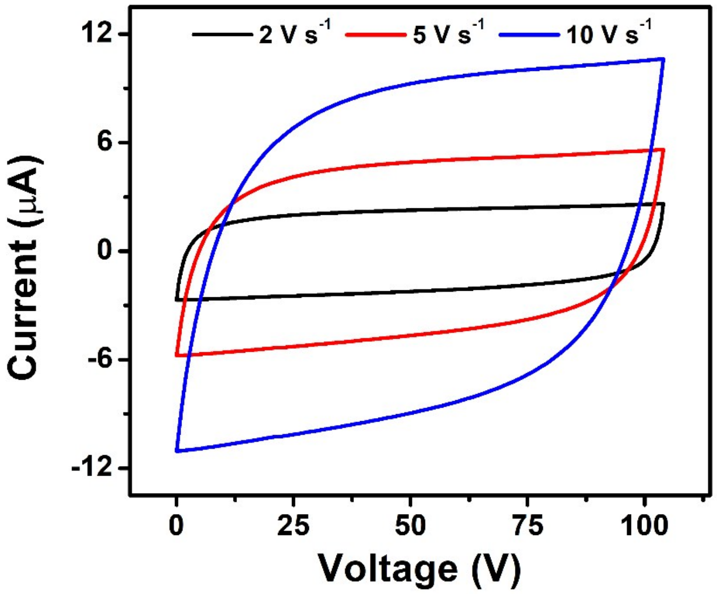

Fig. S21. The CV curves of 104 V SPG-IMSCs, consisting of 130 individual cells, measured at varying scan rates of 2, 5, and 10 V s^{-1}, respectively.

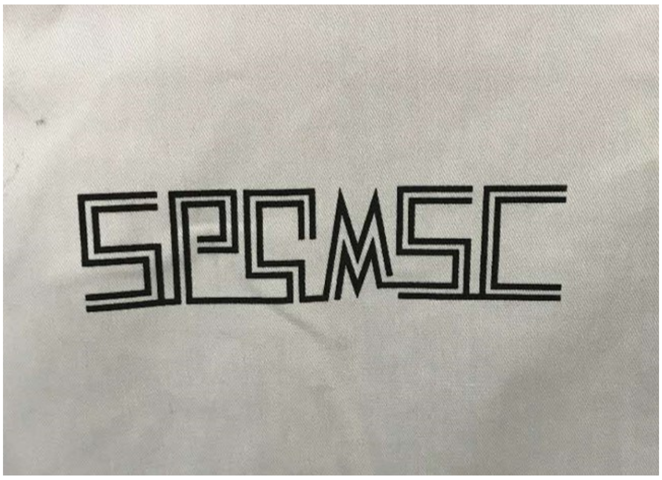

Fig. S22. A photograph of letter-shaped SPG-IMSCs screen printed on lab clothes, demonstrative of wide applicability and great potential of SPG-IMSCs in the direct integration into wearable device systems with our technique.

References:

1. S. Yang, A. G. Ricciardulli, S. Liu, R. Dong, M. R. Lohe, A. Becker, M. A. Squillaci, P. Samori, K. Müllen and X. Feng, *Angew. Chem. Int. Ed.*, 2017, **56**, 6669-6675.
2. S. Barg, F. M. Perez, N. Ni, P. do Vale Pereira, R. C. Maher, E. Garcia-Tunon, S. Eslava, S. Agnoli, C. Mattevi and E. Saiz, *Nat. Commun.*, 2014, **5**, 4328.
3. F. Joucken, Y. Tison, P. Le Fevre, A. Tejeda, A. Taleb-Ibrahimi, E. Conrad, V. Repain, C. Chacon, A. Bellec, Y. Girard, S. Rousset, J. Ghijsen, R. Sporken, H. Amara, F. Ducastelle and J. Lagoute, *Sci. Rep.*, 2015, **5**, 14564.
4. Z. Ben Aziza, H. Henck, D. Di Felice, D. Pierucci, J. Chaste, C. H. Naylor, A. Balan, Y. J. Dappe, A. T. C. Johnson and A. Ouerghi, *Carbon*, 2016, **110**, 396-403.